NANO LETTERS

2006
Vol. 6, No. 4
730−734

Polymeric Nanolayers as Actuators for Ultrasensitive Thermal Bimorphs

Melburne C. LeMieux,[†] Michael E. McConney,[†] Yen-Hsi Lin,[†] Srikanth Singamaneni,[†] Hao Jiang,[‡] Timothy J. Bunning,[‡] and Vladimir V. Tsukruk*[,†]

Department of Materials Science and Engineering, Iowa State University, Ames, Iowa 50011, and Materials and Manufacturing Directorate, Air Force Research Laboratory, Wright-Patterson Air Force Base, Ohio 45433

Received December 22, 2005; Revised Manuscript Received January 30, 2006

ABSTRACT

Polymeric nanolayers are introduced here as active, thermal-stress mediating structures facilitating extremely sensitive thermal detection based upon the thermomechanical response of a bimaterial polymer–silicon microcantilever. To maximize the bimaterial bending effect, the microcantilever bimorph is composed of stiff polysilicon, with a strongly adhered polymer deposited via plasma-enhanced chemical vapor deposition. The polymer layers with thickness ranging from 20 to 200 nm possess a rapid and pronounced response to temperature fluctuations due to intrinsic sensitive thermal behavior. We show that by taking advantage of the thermal stresses generated by the huge mismatch of material properties in the polymer–silicon bimorph, unprecedented thermal sensitivities can be achieved. In fact, the temperature resolution of our bimaterial microcantilevers approaches 0.2 mK with thermal sensitivity reaching 2 nm/mK; both parameters are more than an order of magnitude better than the current metal–ceramic design. This new hybrid platform overcomes the inherently limited sensitivity of current sensor designs and provides the basis to develop the ultimate uncooled IR microsensor with unsurpassable sensitivity.

Enhancing the sensitivity, affordability, and further miniaturization of infrared (IR) detectors[1] is critical for both military and civilian advanced sensor applications ranging from reconnaissance and targeting to medical imaging and weather forecasting.[2] The most effective IR detectors today offer temperature resolution, calculated as the smallest measurable temperature difference, of around 10 mK.[3,4] However, these are primarily photon-detection type sensors that require cryogenic cooling, which drives up the size and cost of the device substantially.[5,6] Thus, rather than relying on a photonic mechanism, the other classification of IR detectors, based on thermal detection, promises to replace photonic devices if similar sensitivity can be achieved.[2,7] To avoid the drawbacks of photon-detection sensors while increasing sensitivity, a new design platform for uncooled thermal detection based on bimorph microcantilever structures has been recently suggested.[8−10] On the other hand, active polymer layers are studied intensively as prospective actuators for many applications.[11]

Microcantilever-based microsensors with organic−polymer layers are readily exploited for chemical and biological analyte detection[12−15] because of their microscopic dimensions, high sensitivity, facile array implementation, and low cost of batch manufacturing.[16] Moreover, their deflection can be monitored by simple optical means with 0.1 Å resolution. A higher impact application, however, is that biomaterial microcantilevers are now the centerpiece in the development of uncooled IR sensors in which several thousands of these miniaturized sensors are packed into MEMS arrays to rival the sensitivity of cooled IR sensors.[2]

In the past few years, bimaterial microcantilevers have been fabricated to serve as uncooled IR sensors.[10] The bimaterial effect works on the following fundamental principal. The interfacial thermal stresses developed within these structures allows for the thermally induced actuation caused by reversible bending deformation of a microcantilever due to a vast mismatch in film properties and thermal expansion coefficients (α) of the materials. The thermal sensitivity of such bimorphs, S, defined as a beam deflection (δ) per a temperature difference depends on geometrical parameters and, most importantly, difference in thermal expansion coefficients of the two materials[3,17]

$$S_{\mathrm{Th}} = \frac{\delta}{\Delta T} = 3(\alpha_{\mathrm{bimat}} - \alpha_{\mathrm{sub}})\left(\frac{n+1}{K}\right)\left(\frac{L_{\mathrm{cant}}{}^2}{d_{\mathrm{sub}}}\right) \quad (1)$$

where L, n, and d are parameters related to beam geometry and K is a structure factor accounting for mechanical

* To whom correspondence should be addressed: vladimir@iastate.edu.
† Department of Materials Science and Engineering, Iowa State University.
‡ Materials and Manufacturing Directorate, Air Force Research Laboratory, Wright-Patterson AFB.

10.1021/nl0525305 CCC: $33.50 © 2006 American Chemical Society
Published on Web 03/11/2006

properties. Ideal bimaterial properties include the following: large mismatch of α and the thermal conductivity (λ) between the two materials, one of the materials should have extremely low λ, the active coating should be applied in a nondestructive deposition, and the absorbing layer may be tuned for a specific IR window.

Barnes and Gimzewski were first to report microfabricated cantilevers coated with a metal to induce effective thermal bending.[17] Majumdar et al. applied bimaterial cantilevers of silicon nitride and gold into a complicated comblike MEMS structure, which resulted in resolution of 3−5 K.[3] Datskos et al. developed a microcantilever bimorph with silicon as a substrate and a 150 nm gold layer coating as the high (α) component that exhibited temperature resolution (minimum detectable temperature difference) of 0.4 K.[18] Recent bimaterial microcantilevers with temperature resolution approaching 5 mK represent the best examples of uncooled IR detectors based on bimaterial microcantilevers.[19] In that design, SiC was the low α component, again being combined with gold as the layer with high thermal expansion.

Still, these sensitivities remain below modern demands due to the inherent limitation in the level of thermally induced stresses for ceramic−metal structures (which is the contemporary design), thus greatly impeding the expansion of uncooled IR sensing technology. This dilemma cannot be resolved within the current selection of materials, and thus a new materials design platform must be implemented into thermal sensor technology. Here, we suggest replacing current ceramic−metal bimorphs with organic−inorganic hybrids to create a bimaterial design with tremendously increased interfacial thermal stresses. These hybrid bimorphs will facilitate microthermal sensors based on a thermomechanical signal transduction with unprecedented sensitivity due to efficient actuation of polymeric layers with nanoscale thickness. The design described here is inspired by an existing efficient and ultrasensitive thermomechanical transduction found in nature. Indeed, the best example of an IR "eye" comes to us from the jewel beetle (*Melanophila acuminata*), which can sense heat from a forest fire 80 km away.[20] The beetle accomplishes this through microscale thermal sensors comprised of alternating hard/compliant nanolayers exploiting a thermomechanical mechanism.[21,22]

Considering that the difference in thermal expansion coefficients for current metal−ceramic bimaterial designs is inherently limited ($\Delta\alpha < 20 \times 10^{-6}$ K^{-1}),[18] the novel polymer−ceramic bimaterial suggested here dramatically enhances thermally induced bending due to a much more efficient actuation of readily expandable polymer nanolayers. We demonstrate that the strongly attached polymer on polysilicon, with $\Delta\alpha \geq 200 \times 10^{-6}$ K^{-1}, combined with low thermal conductivity allows for the ultimate actuation of bimaterial microcantilevers tremendously exceeding current values. Moreover, the fabrication of these bimorphs via room-temperature plasma-enhanced chemical vapor deposition (PECVD)[23,24] is fully compatible with silicon MEMS fabrication technology, thus, facilitating batch manufacturing.[25] The PECVD process is very advantageous here considering the necessity to combine the deposition process with microfabrication manufacturing.

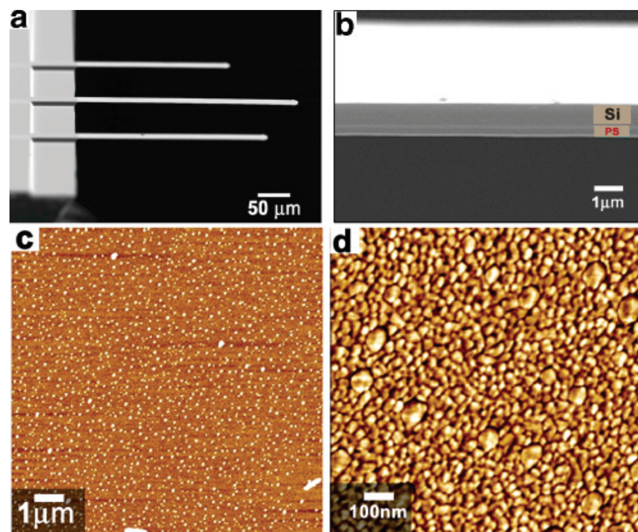

Figure 1. (a) SEM image of the polymer−silicon bimaterial microcantilever. (b) Higher resolution SEM image of the microcantilevers showing the 200 nm PS layer (bottom layer). (c, d) AFM tapping mode images of surface morphology of polymer layer at different magnifications. *Z* scale is 10 nm.

To form model organic−inorganic hybrid bimorphs, silicon microcantilevers commonly utilized as probes for an atomic force microscope (AFM) (300 μm in length, spring constant is 0.06 N/m) were coated with plasma-polymerized polystyrene (PS) via PECVD (see methods) (Figure 1a,b).[26] The PECVD deposition process selectively coats *only* one side of the microcantilever with controllable thicknesses of the highly cross-linked PS layers in the range of 20−200 nm as confirmed with SEM and ellipsometry (Figure 1a,b). Several other monomers such as acrylonitrile and pentafluorostyrene showed comparable results as well and will be discussed in a forthcoming publication. AFM imaging revealed a smooth surface morphology of the polymer surface with a fine, granular nanodomain texture in which root mean square (rms) roughness did not exceed 3 nm indicating uniform surface morphology (Figure 1c,d). The PECVD polymer deposited is a reasonably stiff, highly cross-linked material with the elastic modulus close to 2 GPa as measured by AFM force measurements[27] (full elasticity results will be shown in a forthcoming publication) and cannot be dissolved or swollen in organic solvents.[24]

Upon heating, the polymer−polysilicon beam bends downward reaching a planar state at 40 °C as demonstrated in a side-view optical image in Figure 2. Real-time video of microcantilever deflections in the course of thermal cycling presented in the Supporting Information demonstrates a high level of reversible bending across a wide temperature range with 50 μm reversible deflection occurring. An initial prebent state is introduced in the course of polymer deposition due to chemical reaction inducing the usual compressive residual stresses of PECVD polymers on one side (bottom in Figure 2) of the microcantilever which creates additional tensile stresses. Such a phenomenon leads to a prebent and

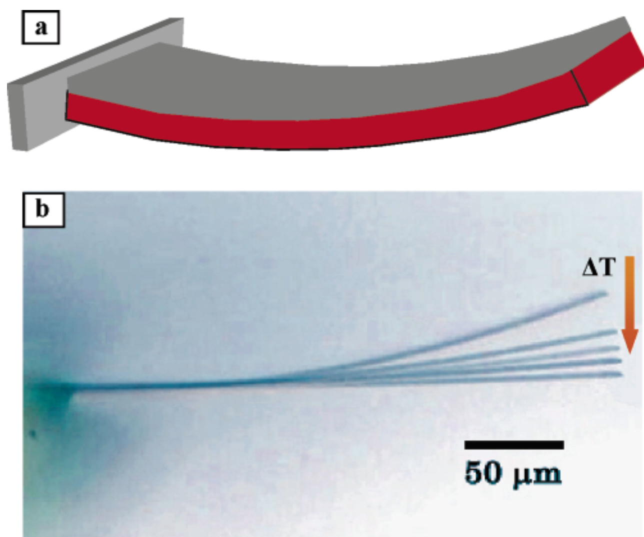

Figure 2. Schematic of the bimaterial cantilever bending upon incident heat (a). Actual optical image (b, side view) of the polymer−silicon microcantilever bending as temperature increases from 20 to 40 °C (see Supporting Information for real time video of thermal bending cycles).

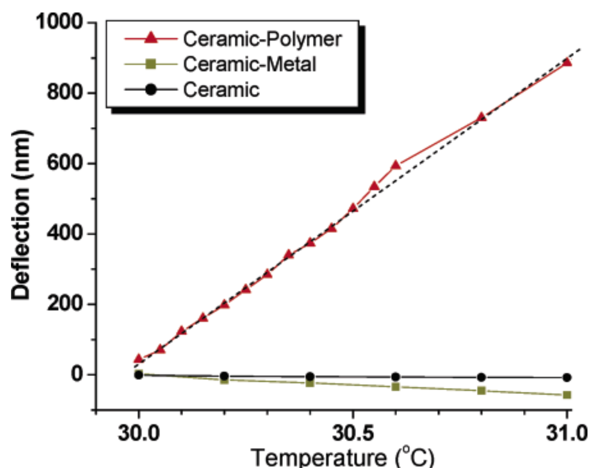

Figure 3. The thermal deflection of microcantilevers within a narrow temperature interval: comparison of polymer−silicon, metal−silicon, and bare silicon microcantilevers. Dash line shows linear fit used to calculate the thermal sensitivity.

prestressed bimorph beam with initial parameters controlled by deposition conditions.[3,28]

To quantify the phenomenon observed, we conducted precise measurements of the microcantilever deflections (with accuracy ±0.05 nm) within a narrow temperature interval and small temperature increments of 50 mK (Figure 3). We compared these data to the reference ceramic−metal microcantilever, which in this case is polysilicon with a 60 nm gold layer (Figure 3). As obvious from this plot, the thermomechanical bending of the polymer−ceramic microcantilever is *many times* higher than the deflection of the reference ceramic−metal microcantilever. The thermal sensitivity reaches 1 nm/mK which is much higher than that for a corresponding gold−polysilicon microcantilever (0.056 nm/mK). The thermal sensitivity achieved here for the polymer−polysilicon bimorph is well beyond the value of 0.12 nm/mK achieved for the best uncooled IR detector employing microcantilevers.[19] Moreover, the direction of thermally initiated deflection is *opposite* to that detected for the gold−polysilicon reference microcantilever, which points out the complex nature of bending of polymer−silicon composite beams as will be discussed below.

In fact, the presence of the polymer layers generates a bending stresses (σ_s) given by a modified Stoney's equation[29,30]

$$\sigma = \frac{E{t_s}^2}{6R(1-\upsilon)t_f} \tag{2}$$

where E is the elastic modulus, t_s is the substrate thickness, R is the radius of curvature, υ is Poisson's ratio, and t_f is the polymer layer thickness. This equation is valid for bicomposite beams and describes interfacial stresses in bent beams. On the other hand, the PECVD-deposited polymer layer creates intrinsic stress associated with grafting, chemical reaction, and growth of polymer layer, σ_i, which is compressive.[31] At room temperature, the microcantilever is in a stable prebent state with balanced stresses

$$\sigma_s - \sigma_i - \sigma_T = 0 \tag{3}$$

where σ_T is the thermal stress (generating additional compression on polymer layer) caused by mismatch of the thermal expansion coefficients of polymer and silicon layers. Considering that $\sigma_T = 0$ at room temperature (PECVD was conducted at room temperature), we can conclude that $\sigma_s = \sigma_I$, and thus use eq 2 for the estimation of the intrinsic compressive stresses. This estimation gives σ_i = 85 MPa, which is a very high value indicating high compression of the polymer layer at room temperature caused by preparation conditions. The high cross-link density of the PECVD polymer layer and their chemical grafting at the interface should provide for enhanced mechanical and thermal stability of these layers even under such high stress.[23,32] Calculation of the differential surface stresses (σ_d) under given conditions according to the simplified Stoney's equation[29,33] gives a value of 10 N/m, which is higher than stresses usually generated by grafting of monomolecular organic layers (usually within 0.3−5 N/m) and resulting from molecular adsorption (<0.2 N/m).[34] Finite element analysis (FEA) of the prebent state of the microcantilevers confirmed this estimation and gives σ_d = 12 N/m. Moreover, it shows that compressive stress within the polymer layer reaches 56 MPa and is balanced by the tensile stress exactly at the polymer−silicon interface of 55 MPa combined with 30 MPa compression stress at the bare silicon surface.

Restoring the planar shape of the microcantilevers at elevated temperature (40 °C for the microcantilever in Figure 2) indicates balanced stresses (eq 3) with $\sigma_s = 0$ (no bending in this state) but nonzero thermal stresses σ_T. This result leads us to the conclusion that the intrinsic stress at the elevated temperature should compensate for both initial intrinsic stress and thermally induced stress. Considering that both stresses

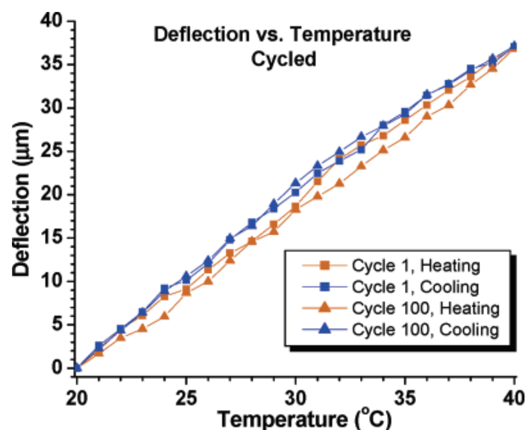

Figure 4. The thermal deflection of microcantilevers within a large temperature interval: heating and cooling cycle summary of 100 runs. Shown in the plot are the initial run and the 100th (final) cycle.

are compressive in nature and act in the same direction, we must conclude that the intrinsic stress within the polymer layer actually *reverses sign* at elevated temperature and becomes tensile, a very intriguing phenomenon. Although a full understanding of this complex thermomechanical behavior requires further detailed studies, it is worth noting that, indeed, a similar phenomenon of changing from compression to tensile stress was observed for PECVD layers and was associated with the changing radical density within the layer leading to material contraction at elevated temperatures.[31] However, in our case, the phenomenon observed is completely reversible as will be demonstrated below.

In fact, to test the reversibility and limits of the polymer−ceramic microcantilever performance, multiple thermal cycling tests were done over a large temperature range with the microcantilevers subjected to heat−cool cycles (Figure 4). The reproducibility of thermal bending under these conditions was quite convincing as the overall fluctuation between the first and last (100th) cycle was less than 5%. The overall thermal sensitivity (slope of the plot in Figure 4) remains constant within 1%. This stability is excellent considering that the total microcantilever deflections reached nearly 50 μm, corresponding to a 1.1% strain that is quite high for silicon. Remarkably, over this temperature range, the thermal sensitivity was found to be 1.86 nm/mK. This sensitivity value is *more than 30 times higher* than that for the reference gold−silicon microcantilever. Moreover, the temperature resolution or minimum detectable temperature difference of these microcantilevers is 0.2 mK, which is an order of magnitude better than that of the best uncooled IR sensors.[2] The sensitivity is limited by thermal vibrations, which have amplitudes of 0.4 $\pm$ 0.1 nm as measured by thermal tuning in air.[35]

In conclusion, the approach described here clearly opens the way for the microfabrication of highly sensitive microscale thermal arrays for miniature thermal imagers with record thermal sensitivity of about 2 nm/mK and the lowest limit of temperature detection of about 0.2 mK. This new hybrid polymer−silicon platform suggested here overcomes the inherently limited sensitivity of current sensor designs and provides the basis to develop the ultimate uncooled thermal sensor with tremendously enhanced sensitivity. In addition, the plasma-deposited organic precursors suggested here expose the delicate microcantilevers to minimal stresses, while easily and rapidly creating nanoscale polymer coatings utilizing a "dry" process compatible with batch microfabrication manufacturing. Due to the wide variety of monomers that can be plasma deposited, our approach allows for further chemical modification to make multifunctional chemical−thermal microsensor arrays with tunable spectral response.

Methods. Materials. The microcantilevers were rectangular (MicroMasch USA, Portland, OR) AFM tips with the following dimensions: $L = 200{-}350\ \mu$m; $W = 20{-}35\ \mu$m; $T = 0.7{-}1.3\ \mu$m as verified by SEM (JEOL JSM-606LV). The tips were uncoated (bare) silicon, while the "reference" tip was silicon with a roughly 60 nm Au layer coated by the manufacturer. Spring constants varied from 0.01 to 0.2 N/m, as measured by the thermal tune method and resonance frequency.[36] Styrene monomer was purchased from Aldrich and bubbled with argon gas to remove oxygen prior to being inserted into the PECVD system.

PECVD. The cantilevers were reversibly mounted on the corresponding wafer, and placed in the PECVD reaction chamber so that only one side of the cantilever was coated. The PECVD chamber is custom built, and details of the system are published elsewhere.[37] Briefly, argon (50−200 cm^3/min, 99.999%), used as the noble gas for generating a plasma, flows into a 10 cm diameter reactor at 0.5−1 Torr vacuum through a capacitively coupled radio frequency (rf, 13.56 MHz) discharge of 5−30 W power. The plasma density is controlled to approximately 108 cm^{-3} in the afterglow region. The precursor gas/vapor is added 20 cm downstream from the plasma generation zone. The substrate is located about 1−3 cm further downstream from the precursor inlet. The distance between the substrates and the inlet of precursor materials can be changed as the requirements of the resulting films change. Precursor flow rates of 0.5 and 1.125 cm^3/min were utilized for the coatings. Films of each polymer were deposited on the microcantilevers, silicon wafers (for ellipsometry and AFM characterization), and IR transparent salt plates for FTIR measurements. AFM measurements were conducted in tapping mode on Dimension 3000 and Multimode microscopes according to the usual routine.[38]

Sensitivity of the Microcantilevers. The response to thermal flux was monitored using a custom-built heating stage to heat the mounted tip, and the corresponding deflection was measured by the Multimode AFM optical system. The tip was brought into a grooved Peltier heating element (Supercool, Göteborg) that was 1.2 cm^2. The laser in AFM systems can heat the tip slightly, and this was factored out of the sensitivity measurements by allowing the system to equilibrate for 30 min. After this time allotment, deflection remained completely constant. The Peltier element was controlled by an ILX Thermo-Controller (ILX, Bozeman, MT) that had 0.001 °C resolution, a range of −50 to 250 °C, and 24 h thermal stability of $\pm$0.005°. The entire setup was enclosed in a small (5 $\times$ 5 $\times$ 10 cm) plastic

enclosure to prevent heat dissipation and to shield against wind forces and noise. The corresponding deflection was measured in voltage deflection on the photodiode and converted into nanometers after the sensitivity of the system (tip, piezo, photodiode) was measured in contact mode AFM. The effect of the laser beam was tested on an unmodified microcantilever, and only long-time random deflections on a nanometer scale have been observed confirming minimum influence of the laser beam. On the other hand, all deflection measurements have been taken at a given temperature after several minutes of equilibration, and even long (hours) waiting did not affect deflection despite exposure to the laser beam. Theoretical thermal deflections have been estimated with FEA using the Structural Mechanics module from COMSOL Multiphysics 3.2.[39] A typical FEA involves the reduction of the energy functional (E) of individual elements of the model. The bimaterial structure was meshed into ~40 000 elements.

Acknowledgment. The authors thank Kyle Anderson for technical assistance and Dr. L. Zhang (Agiltron, Woburn, MA) for technical discussions. Support is provided by AFOSR, F49620-03-C-0069 Grant via Agiltron, Inc., and the AFRL.

Supporting Information Available: Details of the microcantilevers used and real time video of microcantilever deflection. This material is available free of charge via the Internet at http://pubs.acs.org.

References

(1) Kayes, R. J. *Optical and Infrared Detectors;* Springer-Verlag: Berlin, 1977.
(2) Rogalski, A. *Prog. Quantum Electron.* **2003**, *27*, 59−210.
(3) Zhao, Y.; Mao, M.; Horowitz, R., Majumdar, A.; Varesi, J.; Norton, P.; Kitching, J. *J. MEMS* **2002**, *11*, 136−146.
(4) Datskos, P. G.; Lavrik, N. V.; Rajic, S. *Rev. Sci. Instrum.* **2004**, *75*, 1134−1148.
(5) Rogalski, A. *Infrared Phys. Technol.* **1994**, *35*, 1−21.
(6) Henini, M.; Razeghi, M. *Handbook of Infrared Detection Technologies;* Elsevier Sciences Inc: New York, 2002.
(7) Rogalski, A. *Infrared Detectors*; Gordon & Breach: Amsterdam, 2000.
(8) Barnes, J. R.; Stephenson, R. J.; Woodburn, C. N.; O'Shea, S. J.; Welland, M. E.; Rayment, T.; Gimzewski, J. K.; Gerber, Ch. *Rev. Sci. Instrum.* **1994**, *65*, 3793−3798.
(9) Berger, R.; Gerber, C.; Lang, H. P.; Gimzewski, J. K. *Microelectron. Eng.* **1997**, *35*, 373−379.
(10) Senesac, L. R.; Corbeil, J. L.; Rajic, S.; Lavrik, N. V.; Datskos, P. G. *Ultramicroscopy* **2003**, *97*, 451−458.
(11) Tsukruk, V. V. *Prog. Polym. Sci.* **1997**, *22*, 247. Jiang, C.; Markutsya, S.; Pikus, Y.; Tsukruk, V. V. *Nat. Mater.* **2004**, *3*, 721.
(12) Ziegler, C. *Anal. Bioanal. Chem.* **2004**, *379*, 946−959.
(13) Pinnaduwage, L. A.; Gehl, A.; Hedden, D. L.; Muralidharan, G.; Thundat, T.; Lareau, R. T.; Sulchek, T.; Manning, L.; Rogers, B.; Jones, M.; Adams, J. D. *Nature* **2003**, *425*, 474.
(14) Hilt, J. Z.; Gupta, A. K.; Bahir, R.; Peppas, N. A. *Biomed. Microdevices* **2003**, *5*, 177−184.
(15) Hagleitner, C.; Hierlemann, A.; Lange, D.; Kummer, A.; Kerness, N.; Brand, O.; Baltes, H. *Nature* **2001**, *414*, 293−296.
(16) Datskos, P. G.; Oden, P. I.; Thundat, T.; Wachter, E. A.; Warmack, R. J.; Hunter, S. R. *Appl. Phys. Lett.* **1996**, *69*, 2986−2988.
(17) Barnes, J. R.; Stephenson, R. J.; Welland, M. E.; Gerber, C.; Gimzewski, J. K. *Nature* **1994**, *372*, 79−82.
(18) Corbeil, J. L.; Lavrik, N. V.; Rajic, S.; Datskos, P. G. *Appl. Phys. Lett.* **2002**, *81*, 1306−1308.
(19) Hunter, R. S. *Proc. SPIE* **2003**, *5074*, 469−480.
(20) Hazel, J.; Fuchigami, N.; Gorbunov, V.; Schmitz, H.; Stone, M.; Tsukruk, V. V. *Biomacromolecules* **2001**, *2*, 304−312.
(21) Schmitz, H.; Bleckmann, H.; Murtz, M. *Nature* **1997**, *386*, 773−774.
(22) Gorbunov, V.; Fuchigami, N.; Stone, M.; Grace, M.; Tsukruk, V. V. *Biomacromolecules* **2002**, *3*, 106−115.
(23) Kim, M. C.; Cho, S. H.; Lee, S. B.; Kim, Y.; Boo, J. H. *Thin Solid Films* **2004**, *447−448*, 592−598.
(24) Biederman, H. *Plasma Polymer Films;* Imperial College Press: London, 2004.
(25) Zou, X. P.; Kang, E. T.; Neoh, K. G.; Zhang, Y.; Tan, K. L.; Cui, C. Q.; Lim, T. B. *Polym. Adv. Technol.* **2001**, *12*, 583−595.
(26) Jiang, H.; O'Neill, K.; Grant, J. T.; Tullis, S.; Eyink, K.; Johnson, W. E.; Fleitz, P.; Bunning, T. J. *Chem. Mater.* **2004**, *16*, 1292−1297.
(27) Chizhik, S. A.; Huang, Z.; Gorbunov, V. V.; Myshkin, N. K.; Tsukruk, V. V. *Langmuir* **1998**, *14*, 2606. Tsukruk, V. V.; Huang, Z. *Polymer* **2000**, *41*, 5541.
(28) McFarland, A. W.; Poggi, M. A.; Doyle, M. J.; Bottomley, L. A.; Colton, J. S. *Appl. Phys. Lett.* **2005**, *87*, 053505.
(29) Dareing, D. W.; Thundat, T. *J. Appl. Phys.* **2005**, *97*, 043526.
(30) Chen, J.; De Wolf, I. *Semicond. Sci. Technol.* **2003**, *18*, 261.
(31) Morinaka, A.; Asano, Y. *J. Appl. Polym. Sci.* **1982**, *27*, 2139.
(32) Denes, F. S.; Manolache, S. *Prog. Polym. Sci.* **2004**, *29*, 815−885.
(33) Wu, G.; Ji, H.; J.; Hansen, K.; Thundat, T.; Datar, R.; Cote, R.; Hagan, M. F.; Chakraborty, A. K.; Majumdar, A. *Proc. Natl. Acad. Sci. U.S.A.* **2001**, *98*, 1560−1564.
(34) Godin, M.; Williams, P. J.; Tabard-Cossa, V.; Laroche, O.; Beaulieu, L. Y.; Lennox, R. B.; Grütter, P. *Langmuir* **2004**, *20*, 7090.
(35) Sader, J. E.; Chon, J. W. M.; Mulvaney, P. *Rev. Sci. Instrum.* **1999**, *70*, 3967−3969.
(36) Hazel, J. L.; Tsukruk, V. V. *Thin Solid Films*, **1999**, *339*, 249.
(37) Haaland, P.; Targove, J. *Appl. Phys. Lett*. **1992**, *61*, 34−36.
(38) Tsukruk, V. V. *Rubber Chem. Technol.* **1997**, *70*, 430. Tsukruk, V. V.; Reneker, D. H. *Polymer* **1995**, *36*, 1791.
(39) *Structural Mechanics Module Model User's Guide for Femlab3*; COMSOL AB: Stockholm, Sweden, 2004.

NL0525305